Newcastle University

ePrints

Bai D, Benniston AC, Tkachenko NV, Lemmetyinen H, Whittle V. ROFRET: A Molecular-Scale Fluorescent Probe Displaying Viscosity Enhanced Intramolecular Förster Energy Transfer. *ChemPhysChem* 2014, 15(14), 3089-3096.

Copyright:

This is the peer reviewed version of the following article: Bai D, Benniston AC, Tkachenko NV, Lemmetyinen H, Whittle V. ROFRET: A Molecular-Scale Fluorescent Probe Displaying Viscosity Enhanced Intramolecular Förster Energy Transfer. *ChemPhysChem* 2014, **15**(14), 3089-3096., which has been published in final form at http://dx.doi.org/10.1002/cphc.201402320. This article may be used for non-commercial purposes in accordance with Wiley Terms and Conditions for Self-Archiving.
http://www.interscience.wiley.com/

DOI link to article:

http://dx.doi.org/10.1002/cphc.201402320

Date deposited:

20/05/2015

This work is licensed under a Creative Commons Attribution-NonCommercial 3.0 Unported License

Newcastle University ePrints - eprint.ncl.ac.uk

ROFRET: A molecular-scale fluorescent probe displaying viscosity enhanced intramolecular Förster energy transfer

Dan Bai,[a] Andrew C. Benniston,[a]* Victoria L. Whittle,[a] Helge Lemmetyinen[b] and Nikolai V. Tkachenko[b]*

Abstract: The fluorescent probe **ROFRET** contains a Bodipy molecular rotor connected via a short triazole-based spacer to a fully alkylated Bodipy. Förster resonance energy transfer takes place from the rotor to the other Bodipy, and is enhanced to a limiting value as the viscosity of the solvent increases. Time-resolved spectroscopy and steady-state studies are consistent with both a forward and reverse energy transfer, and delayed fluorescence.

Keywords: Bodipy • viscosity• rotor • energy transfer • Förster

[a] Prof A. C. Benniston, Dr V. L. Whittle and Dr Dan Bai
Molecular Photonics Laboratory
School of Chemistry
Newcastle University, Newcastle upon Tyne, NE1 7RU, UK
Fax: (+44) 191 222 6929
E-mail: a.c.benniston@ncl.ac.uk

[b] Prof H. Lemmetyinen and Prof N. V. Tkachenko
Department of Chemistry & Bioengineering
Tampere University of Technology, PO Box 541
33101, Tampere, Finland.

Supporting information for this article is available on the WWW under http://www.chemeurj.org/ or from the author.

Introduction

Molecular environment-sensitive probes offer the opportunity to chart physical and structural alterations on the nanoscale.[1] Many areas of science have benefited from the unique information afforded by probes located within inaccessible spaces, which could not be collected by conventional techniques.[2] Response to pH,[3] polarity,[4] temperature,[5] extraneous metal ions,[6] poisons[7] and biomolecules[8] are common place. Luminescence has certainly been one of the most popular methods used for readout purposes, since it is highly sensitive and non-intrusive when employed for biological applications.[9] Temporal profiling is also possible with luminescence, so that timescales (e.g., picoseconds to milliseconds) for molecular events are achievable.[10] There are a wealth of fluorescent reporters to date, some of which are tailor-made for specific purposes such as reactive oxygen species (ROS) detection,[11] lipid mobility monitoring,[12] protein sequencing[13] and DNA/RNA recognition.[14] Certainly one of the most versatile classes of fluorescent reporters to date is based on the boron dipyrromethene (Bodipy) group.[15] Generally, the fully alkylated molecule is strongly fluorescent in fluid solution at room temperature.[16] It is very noticeable that fluorescence is much lower for certain fully non-alkylated versions, especially in non-viscous solvents.[17] There is an enhancement (ca. 4 fold) in fluorescence quantum yield as the solvent viscosity increases by around 10 cP. The solvent viscosity effect is traced to a reduction in the non-radiative decay process, and the retardation in rotation of the meso aryl group with the increase in solvent viscosity.[18] As the aryl group

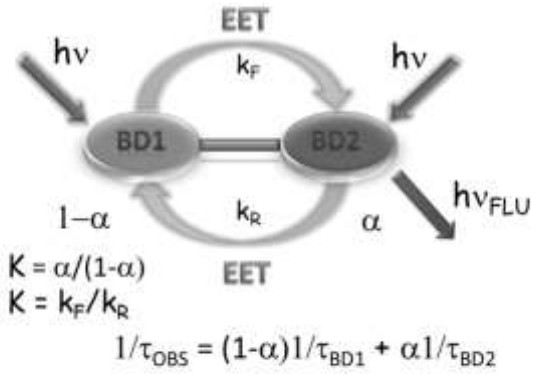

Scheme 1. Simple cartoon representing forward and reverse EET in a Bodipy-based dyad and the partition coefficient α. The equilibrium constant (K) is defined in terms of α and the rates for forward and reverse energy transfer.

rotates it distorts slightly the dipyrromethene backbone, which in turn affects the rate for non-radiative decay. The one problem with the first prototype so-called Bodipy molecular rotor was its low starting point fluorescence output. We were especially interested to see if the original signal could be enhanced, with no detrimental effect on the overall fluorescence viscosity response. It is documented that the absorption maximum for non-alkylated Bodipy derivatives (e.g., **ROT**) occurs at higher energy compared to the alkylated version, **BD**.[19] Emission from **ROT** as a result overlaps particularly well with the absorption profile for **BD**. From basic theory efficient electronic energy transfer (EET) is expected between the two groups at separation distances less than the Förster radius ($R<R_0$).[20] For the designed dyad, **ROFRET**,[21] the triazole-alkyl spacer separates the two Bodipy groups by ca. 17Å, and electronically decouples the groups (Figure 1). At a simple level, the working of **ROFRET** relies on the rotor Bodipy sensitizing emission for **BD**, so that the more fluorescent Bodipy is now the reporter. There is also the interesting scenario where emission from **BD** overlaps to a small extent with absorption for **ROT**. Thus, reverse Förster EET is feasible,[22] especially since the fluorescence quantum yield for **BD** alone is high. Under these conditions the case would arise whereby the two Bodipy groups fluoresce with a common lifetime, and partitioning of energy between them is dependent on the rates for forward (k_F) and reverse (k_R) energy transfer (Scheme 1).[23] It is worth noting that at very short timescales after excitation the system is at non-equilibrium and attains equilibrium with a rate equal to $k_F + k_R$.[24] The case is very reminiscent of that seen for linked pyrene-Ru(II)polypyridyl dyads.[25] Fluorescence spectra recorded for **ROFRET** in a series of alkanol solvents showed a steady increase in quantum yield but reached a plateau at around pentanol. The behaviour is different to simply **ROT** alone, and the dyad appears to only work over a narrow viscosity range. A positive feature is the much lower concentration of the probe needed to collect a reasonable output signal. This is certainly an advantage for the monitoring of fluorescence in environments where high dye concentration may cause cross signal contamination by intermolecular interactions.

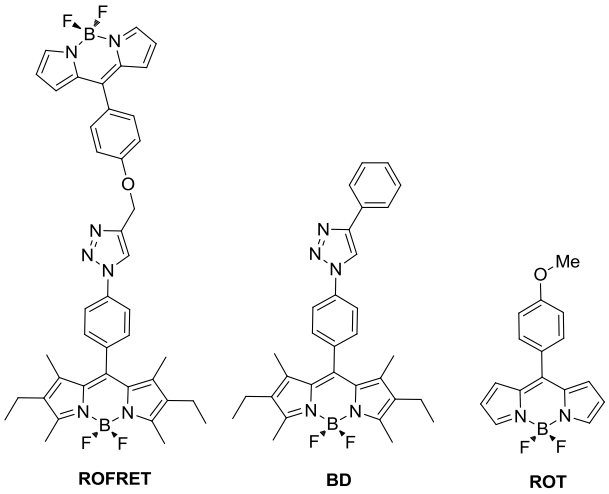

Figure 1. Chemical formulae of Bodipy compounds discussed in the main text.

Results and Discussion

Synthesis and Molecular Structure

The preparation of the molecular dyad is shown in Scheme 1 (see Experimental), and involves coupling the azide **1** with the acetylene derivative **2** using "click chemistry".[26] The final material was extensively purified by column chromatography to afford **ROFRET** in 87% yield as a red solid. Analytical techniques including NMR spectroscopy (^{1}H, ^{13}C, ^{19}F, ^{11}B) and mass spectrometry were consistent with the final structure. Both ^{11}B and ^{19}F NMR spectra revealed the presence of two slightly different Bodipy units. The chemical shifts for the boron and fluorines for the rotor part are shifted downfield with respect to the fully alkylated Bodipy. The clear singlet at 8.20 ppm in the ^{1}H NMR spectrum is readily assigned to the triazole group.

From inspection of **ROFRET** it is evident that the rotor Bodipy is susceptible to free rotation about the methylene connector. A basic precession cone is expected which will bring the rotor into close proximity to the reporter Bodipy. An energy-minimised structure calculated using Gaussian 03[27] and DFT (B3LYP) and a 6-311G basis set (see Supporting Information) places the two subunits ca. 17 Å apart. A more insightful picture into molecular conformations was obtained by commencing with the energy-minimised structure, and through a series of scan steps, altering the dihedral angle at the oxygen atom. To reduce computer run time the basis set was reduced to 3-21G (B3LYP). Further refinement involved minimising the energy of the structure at each dihedral angle. In this way a profile was constructed containing a series of structures for which the intramolecular **BD** to **ROT** separation distance varied (see Supporting Information). The energy difference between, for example, two conformations where the separation distances are 10.7 Å and 17.3 Å is only 5 kcal mol^{-1}. We infer from the calculations that **ROFRET** is flexible enough to permit **BD** and **ROT** to easily sample numerous separation distances in fluid solution. In case of inter chromophore energy transfer this variation in distance suggests that the transfer time constant may differ as much as 20 times for different conformers.

Absorption and Fluorescence

The electronic absorption spectrum for **ROFRET** in MeOH is shown in Figure 2. The overall profile is a convincing superimposition of the absorption spectra for the two control compounds **BD** and **ROT** under identical conditions. The two main intense peaks at low-energy are the S_0-S_1 electronic transitions for the Bodipy. The peak maxima (λ_{ABS}) are 497 nm and 524 nm, respectively. As seen previously, the HOMO-LUMO gap is affected by substitution of alkyl groups on the dipyrromethene backbone.[28] The energy gap is reduced by ca. 1000 cm^{-1} so that two clear maxima are observed for the two components. There is still appreciable overlap of bands (in the range 450 - 500 nm) from both components to render selective excitation of a single chromophore problematic.

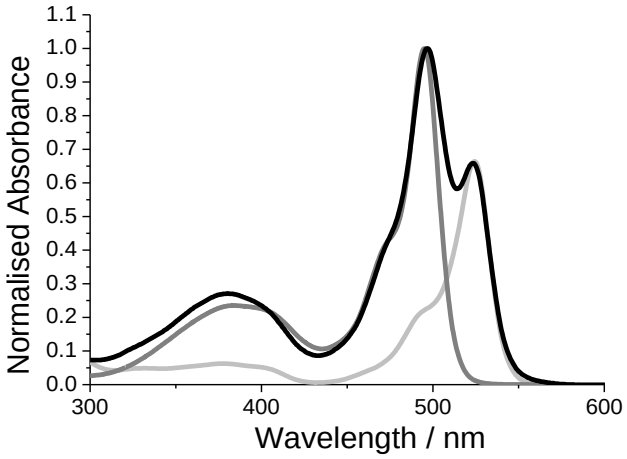

Figure 2. Room temperature normalised absorption spectra for **ROFRET** (black) , **BD** (light grey) and **ROT** (dark grey) in MeOH.

The fluorescence spectrum collected for a 1:1 mixture of **BD** and **ROT** in dilute MeOH, excited at 470 nm, is dominated by a profile centred at λ_{EM} = 542 nm. A small shoulder is also seen situated at around 515 nm. The long wavelength band is assigned to emission from **BD**, while the shoulder is from **ROT**. The fully corrected fluorescence excitation spectrum is a poor match of the absorption profile (see Supporting Information). The spectrum resembles that observed for **BD** alone. The quantum yield of fluorescence (ϕ_{FLU}) for isolated **BD** is about 16 times larger than **ROT** in dilute MeOH at room temperature. At the excitation wavelength **BD** absorbs only ca. 25% of the photons. Therefore, the fluorescence intensity for **BD** should be about 4 times larger than for **ROT** assuming the two components are non-interacting. The observed difference is somewhat similar, which suggest that intermolecular energy transfer between **BD** and **ROT** is negligible. The emission spectrum for **ROFRET** is again dominated by a sharp band at 542 nm, but the possible shoulder at 515 nm is a little more difficult to judge. In contrast, the peak is more discernible in OctOH (n-octanol), especially when compared to **BD** in the same solvent (see Supporting Information). Contrary to the 1:1 mixture case, the fully corrected fluorescence excitation spectrum for **ROFRET** in MeOH (and OctOH) matches well with the absorption profile over a wide spectral range (see Supporting Information). The measured ϕ_{FLU} is 0.17 and fluorescence lifetime (τ_s) in MeOH is 3.0 ns. Collected in Table 1 are values for ϕ_{FLU} and τ_s for **ROFRET** and the control compounds in the other solvents. The cumulative evidence supports the notion of efficient intramolecular energy transfer from **ROT** to **BD**.

Table 1. Photophysical data for **ROFRET**, **BD** and **ROT** in alkanol solvents.

Compound	Solvent	MeOH	BuOH	OctOH
ROFRET	ϕ_{FLU}	0.17	0.26	0.28
	$\tau_{s\,/}$ ns	3.0	3.9	4.8
BD	ϕ_{FLU}	0.63	0.60	0.72
	τ_s / ns	5.1	5.1	5.1
ROT	ϕ_{FLU}	0.038	0.071	0.134
	τ_s /ns	0.32	0.59	0.84

Absorption and fluorescence spectra recorded for **ROFRET** in other alkanol solvents were similar to the MeOH case. Any small shifts observed in both λ_{ABS} and λ_{EM} are accounted for by changes in polarizability of the solvents. Again, fluorescence excitation spectra matched extremely well with the absorption spectra, in line with the view of efficient intramolecular energy transfer (see Supporting Information). Fluorescence spectra were also recorded for spin-coated dilute

films of **ROFRET** in PMMA on glass (see Supporting Information). In such a rigid matrix the spinning of the phenylene paddle in the rotor Bodipy is reduced significantly. The ϕ_{FLU} is maximised, but several disparate conformations for **ROFRET** are 'locked' within the rigid matrix. There is evidence for a low-intensity long-wavelength emission at around 700 nm suggesting that a conformer is generated where the two Bodipy units are in close proximity. More distinctive is fluorescence from the rotor Bodipy, indicating conformers exist for which the efficiency of energy transfer is either reduced or delayed fluorescence is enhanced.

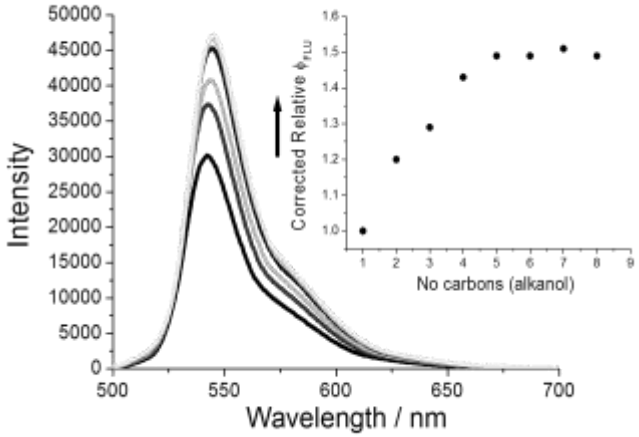

Figure 3. Increase in the fluorescence intensity for **ROFRET** with change in selected alkanol solvents (first-CH_3OH, second-C_2H_5OH, third-C_3H_7OH, fourth-C_4H_9OH, fifth-$C_5H_{11}OH$, sixth-$C_8H_{17}OH$). Insert shows the change in ϕ_{FLU} relative to methanol and corrected for refractive index changes for the solvents.

A distinct increase in ϕ_{FLU} (Figure 3) is noticed for optically matched solutions of **ROFRET** in linear alkanols. Correcting for small changes in the refractive index of the solvents across the series, the relative ϕ_{FLU} increases and reaches a plateau at around pentanol. The same data re-plotted against viscosity shows that a levelling off occurs at around 6 cP. The limiting ϕ_{FLU} is ca. 0.28. The dyad **ROFRET** would only appear to respond to a narrow viscosity window. On a positive note the output signal is more discernible than for simple **ROT** alone, since the starting quantum yield is around 4.5 times greater.

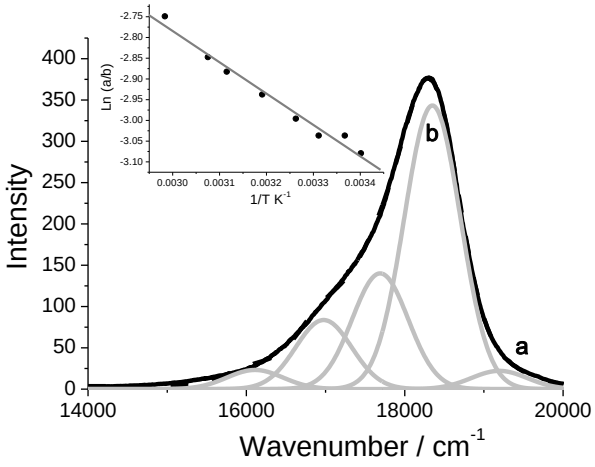

Figure 4. Spectrum for **ROFRET** at 335 K in OctOH and deconvoluted into five Gaussian bands. Insert depicts the natural logarithm of the ratio of areas for the two Gaussian bands a and b with respect to 1/T. Slope = -755 K (R^2 = 0.98).

Temperature Dependence

Fluorescence spectra for **ROFRET** were recorded in OctOH over a modest temperature range (294 K-335 K). Special focus on the shoulder at around 515 nm was made, looking especially for any changes in its intensity with temperature. With increasing temperature the overall fluorescence intensity decreased by ca. 40% and there was no discernible change in $\lambda_{EM;}$ there occurred to be a slight broadening in the band shape at high temperature as expected (see Supporting Information). Under identical conditions similar changes are observed for the control compound **BD**. Part of the alterations in intensity for both Bodipy compounds can be accounted for by the ca. 4% change in density of the solvent, and the modification in concentration of the solutes. Each spectrum for **BD** could be adequately deconvoluted into five Gaussian bands as shown in Figure 4. Recalling that the high-energy tail for each spectrum represents emission from **ROT**, the ratio of areas corresponding to a/b at each temperature showed a clear temperature dependence (Figure 4 insert). Fitting of the data to a basic Boltzmann distribution afforded an energy gap (ΔE) of 525 cm^{-1}. Considering the assumptions, ΔE is in fairly good agreement with the spectroscopic energy gap (900 cm^{-1}), and so part of the emission from **ROFRET** is due to delayed fluorescence.

Spectral Overlap and Reverse Energy Transfer

The emission from **ROT** overlaps extremely well with the absorption profile for **BD** in the three sample solvents (see Supporting Information). The Förster overlap integrals[29] calculated using Eq. 1 for forward EET from **ROT** to **BD** (J^F) are collected in Table 2.

$$J^F = \frac{\int F(\nu)\varepsilon(\nu)\nu^{-4}\delta\nu}{\int F(\nu)\delta\nu} \quad (Eq.1)$$

Here, F(ν) is the fluorescence intensity for **ROT** at wavenumber ν, and ε is the molar absorption coefficient for **BD** at wavenumber (ν). The denominator in the equation is used to normalise the fluorescence data.

The variation in J^F across the alkanol solvent series is rather modest. Interestingly, the low energy tail for emission from **BD** overlaps slightly with the absorption of **ROT** in all the alkanol solvents (see Supporting Information). It is possible to calculate the equivalent overlap integral (J^R) for reverse EET by modification of Eq.1. In this case F(ν) now relates to **BD** and ε is the molar absorption coefficient for **ROT** at wavenumber (ν). The term energy donor and energy acceptor for **ROFRET** is meaningless under such conditions. The values for J^R are around 100 times smaller than J^F for all three solvents. At first it appears that reverse EET need not be considered. However, one point to recognise is the 16 fold difference in fluorescence quantum yields between **ROT** and **BD**. Hence, in calculating the Förster critical distance (R_0) by Eq. 2, where κ^2 is the orientation factor, n is the refractive index, J is the overlap integral and the ϕ_D is the quantum yield of the donor alone, the J x ϕ_D terms for forward and reverse EET become more comparable (Table 2). The difference is about a factor of 10.

$$R_0^6 = \frac{8.8x10^{-25}\kappa^2\phi_D J}{n^4} \quad (Eq.2)$$

Graphically, the results are best represented in terms of the probability for forward (P_F) and reverse (P_R) EET using Eq. 3, at various separation distances R (Figure 5).[30] It is evident that at separation distances under ca. 20 Å the probabilities for both forward and reverse EET are reasonably high (>75%) and they are not too different. In contrast, at large separation distances the discrimination between P_F and P_R is significant to the point where the reverse process is unimportant.

$$P = \frac{{R_0}^6}{R^6 + {R_0}^6} \quad (Eq.3)$$

Table 2. Calculated parameters for Förster energy transfer in various solvents for **ROFRET**.

Solvent	J_F 10^{-13}[d]	J_R 10^{-15}[d]	ϕ_{ROT} x J_F 10^{-14}[d]	ϕ_{BD} x J_R 10^{-15}[d]	R_0^F [e]	R_0^{R}[e]	$(R_0^F/R_0^R)^6$
MeOH[a]	2.6	1.8	1.0	1.2	35	24.5	8.5
BuOH[b]	2.9	2.8	2.1	1.7	38	25	12.3
OctOH[c]	3.2	3.7	4.3	2.7	43	27	16.3

[a] Methanol, [b] n-Butanol, [c] n-Octanol, [d] $mmol^{-1}$ cm^6, [e] calculated for κ^2 =0.66 and using n for the solvents.[31]

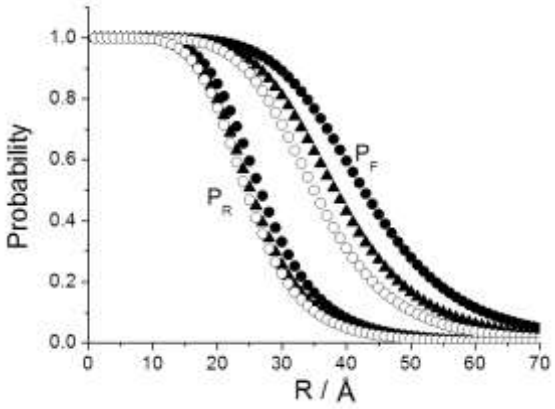

Figure 5. Probability for forward and reverse EET in ROFRET in OctOH (●), BuOH (▲) and MeOH (○).

In the context of Figure 5 it is critical to evaluate the separation distance between the two chromophores in ROFRET. The DFT calculated energy-minimised structure for the dyad places the two Bodipy units *ca.* 17 Å apart. At this separation distance the ratio P_F/P_R varies only slightly from 1.10 (MeOH) to 1.09 (BuOH) and finally 1.06 (OctOH). The maximum separation of the two Bodipy groups is around 19 Å, and the discrimination between P_F and P_R increases somewhat for the three solvents (1.19-MeOH,1.17-BuOH, 1.11-OctOH). Different conformations for ROFRET in solution modulate the probability for intramolecular EET, but the short tether between the two chromophores does mean that the variation in P_F/P_R is rather modest. The effect of the change in P_F/P_R with solvent on the steady-state spectra qualitatively predicts that for moving along the alkanol series: (a) the emission ratios BD/ROT should decrease, and (b) the total emission intensity will increase (see Supporting Information). Both these predictions are experimentally observed.

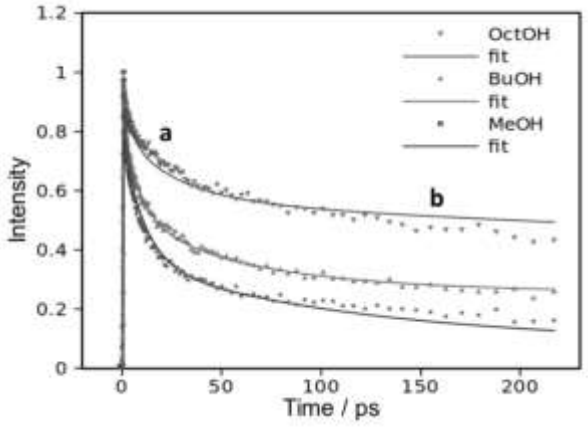

Figure 6. Up-conversion fluorescence decay data collected for ROFRET in octanol (▼), butanol (▲) and methanol (■).

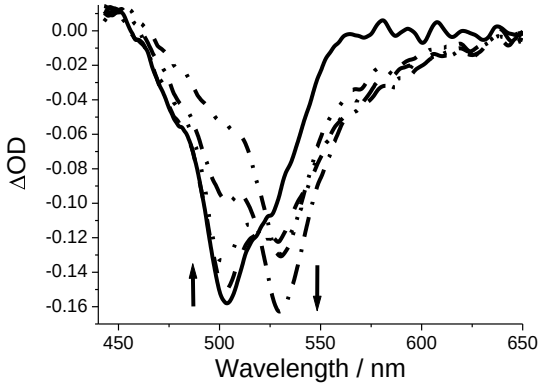

Figure 7. Differential transient absorption spectra recorded at different time delays (1.1 ps (-), 1.8 ps (---), 3.8 ps (····), 35 ps (-·-·-·), 1ns (-·····)) following excitation of **ROFRET** in OctOH with a 70 fs laser pulse at 395 nm**.**

Time-Resolved Spectroscopy

Steady-state fluorescence experiments are in full agreement with intramolecular energy transfer between the two Bodipy units in ROFRET. Based on calculations we should also expect to observe the effect of reverse Förster energy transfer, though one complication is the distribution of conformers from which EET can take place. At a fast timescale probing the conformers are essentially frozen in time and EET events should be represented by a few decay components with lifetimes determined by a distance distribution.[32] Thus, to collect a more complete picture of the temporal events data were collected using both up-conversion spectroscopy and femtosecond pump-probe spectroscopy. Only three solvent systems were studied, and they denote different points on the ϕ_{FLU} correlation curve (Figure 3). The up-conversion emission decay data collected for ROFRET in these three solvents are shown in Figure 6. The monitoring wavelength was set at 500 nm in attempt to selectively collect emission from ROT within the dyad. The first point to note is the fast initial decay (region a) which is followed by a much slower decay (region b) which contributes to ca. 60% of the overall profile for the OctOH case. Changing the solvent to BuOH and finally MeOH afforded similar looking profiles (Figure 6), but the contribution for the long-lived component diminished.

Excitation of **ROFRET** in OctOH with a 70 fs laser pulse delivered at 395 nm resulted in a bleach effect as shown in Figure 7. At the excitation wavelength ca. 30% of photons are absorbed by the **BD** unit in the dyad. At the very early time delay the profile appears to be dominated by bleaching from the rotor Bodipy (502 nm). A closer inspection reveals that there is also a contribution from the **BD** unit in the dyad. With increasing time delays this contribution increases to the expense of reduction in the bleach signal for the rotor Bodipy. At around 1 ns the transient profile appears to be only associated with **BD** from **ROFRET**. However, there is considerable absorption overlap for **BD** and **ROT** in the region around 500 nm.

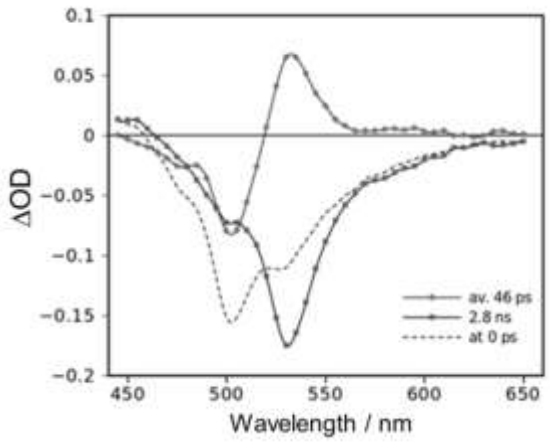

Figure 8. Transient absorption spectrum of ROFRET in OctOH right after excitation (dashed line) and decay component spectra obtained from global fit of transient absorption and emission decays (see text for details).

The quantitative analysis of the time resolved data is complicated by the presence of conformers with different chromophore separation distances, and thus with different energy transfer time constants. Experimentally this is observed as non-exponential conversion form initially bleached **ROT** to bleached **BD** state in transient absorption measurements (Figure 7), and non-exponential emission in 1-100 ps time frame (Figure 6). To model the case the decays were fitted by the sum of exponents with fixed proportion between the exponential components, i.e., $a_1 \exp(-t/\tau_1) + a_2\exp(-t/\tau_2)$, where $a_1 + a_2 = 1$ and a_1 and a_2 do not depend on wavelength. This approach can be justified by the presence of two conformers which have identical spectra but different time constants of energy transfer. Furthermore, this decay function should apply equally well to both emission and transient absorption measurements, since in both cases the determining parameter is the concentration of the excited state. Therefore a global fit was applied simultaneously to emission and absorption data collected in the same solvents. The results of the fit for emission decays are presented by solid lines in Figure 6. An example of transient absorption fit results is shown in Figure 8, where the dashed curve shows time-resolved transient absorption spectrum directly after excitation. This initial spectrum is mostly the **ROT** excited state, and the fast component represents the spectrum associated with an energy transfer transition from mainly excited **ROT** to the **BD** excited state. The final slow component corresponds to predominantly the **BD** excited state. Similar spectra were obtained for two other solvents (see Supporting Information). As expected from estimated dispersion in distances between different conformers, the variance between lifetimes was 10 - 20 times with the faster lifetime being of few picoseconds and the longer close to hundred picoseconds. An average energy transfer time constant was calculated as $\tau_{av} = a_1\times\tau_1 + a_2\times\tau_2$, and was 39 ps in MeOH, 22 ps in BuOH, and 42 ps in OctOH, which is much shorter than the relaxation to the ground state 3 - 5 ns.

Interpretation

The time constant to achieve energy transfer equilibrium depicted in Scheme 1, $\tau_{eq} = (k_F + k_R)^{-1}$, is reasonably shorter than the relaxation time constants of either of the chromophores. Using this information along with lifetime data (Table 1) the partitioning of energy between the two Bodipy chromophores can be evaluated (Table 3). Not too surprisingly the energy is almost exclusively localised on the **BD** unit within **ROFRET**. For quantitative characterization of equilibrium one can introduce the relative concentration of the excited state $\alpha = [BD^*]_{eq}/([BD^*]_{eq} + [ROT^*]_{eq})$, which also can be expressed in terms of ratio of forward and reverse energy transfer rates, $k_F/k_R = \alpha/(1-\alpha)$. Furthermore, the relative concentration can also be used to calculate the total or observed relaxation time constant as:

$\tau_{obs} = ((1-\alpha)/\tau_{ROT} + \alpha/\tau_{BD})^{-1}$ (Eq. 4)

and can be estimated from the lifetimes collected in Table 1. It follows that the energy transfer rate constants are $k_F = \alpha/\tau_{eq}$ and $k_R = (1-\alpha)/\tau_{eq}$ and the results of the calculations are summarized in Table 3.

Table 3. Calculated parameters for **ROFRET** in alkanol solvents

Solvent	α	1-α	K[a]	$k_F\ 10^9$ s^{-1}	$k_R\ 10^9$ s^{-1}
MeOH	0.95	0.05	19	32	1.6
BuOH	0.96	0.04	24	44	1.8
OctOH	0.99	0.01	99	21	0.27

[a] Value calculated from spectroscopic data (Table 1), using the equation shown in Scheme 1 and where $k_F + k_R$ is taken as the fast component from up-conversion spectroscopy.

There is a clear bias towards the photonic energy residing on the **BD** unit as the solvent viscosity increases. Whereas there is a slight variation in k_F with change in viscosity, the reverse energy transfer process is *ca.* 7 fold slower for the OctOH case. Several studies have discussed the effect of solvent viscosity on intramolecular energy transfer in bimolecular reactions and flexible bi-chromophoric assemblies.[33] Brownian dynamics simulations have been used to try and model the fluctuating distance between interacting chromophores, and relate this to Wilemski-Fixman theory.[34] The separation distances between chromophores capable of being sampled in **ROFRET** are considerably shorter than the Förster radius. Thus, any attempt to fully rationalise the viscosity effect is fraught with problems. It is possible that **ROFRET** does not sample the same conformer space in the more viscous OctOH solvent. And as consequence the population of a conformer that facilitates reverse energy transfer is less than in the other two solvent cases.

Conclusion

By using efficient intramolecular energy transfer the dyad **ROFRET** displays viscosity sensitive fluorescence response. The molecular system works differently to a ratiometric dyad viscosity sensor developed by Haidekker and co-workers.[35] Here, the design encompassed the principle of FRET, but two distinctive emission bands could be observed. Emission from one band was independent of local viscosity whereas the other changed. Even though under steady state conditions only a single emission band is observed for **ROFRET** it appears at long wavelength and well away from possible autofluorescence that can hamper data collection in, for example, cell imaging. The “click chemistry” synthetic approach to **ROFRET** also opens

up a simple way to create a rotor viscosity library of dyads, especially sensors with dual responsive behaviour towards, for example, pH[36] and Reactive Oxygen Species (ROS).[37]

Experimental Section

All chemicals were purchased from commercial sources and used as received unless otherwise stated. Basic solvents for synthesis were dried using literature methods. Solvents for spectroscopic investigations were of the highest purity available. All preparations were carried out under N_2 unless otherwise stated. The preparation of **ROFRET** is shown in Scheme 2. Compounds **1** and **2** were available from previous studies. Details for spectroscopic measurements are found in Supporting Information. Computational calculations were performed using a 32-bit version of Gaussian 03 on a quadruple-core Intel Xeon system with 4GB RAM. The calculations were run in parallel, fully utilising the multi-core processor. Energy minimisation calculations were monitored using Molden and run in parallel with frequency calculations to ensure optimised geometries represented local minima.

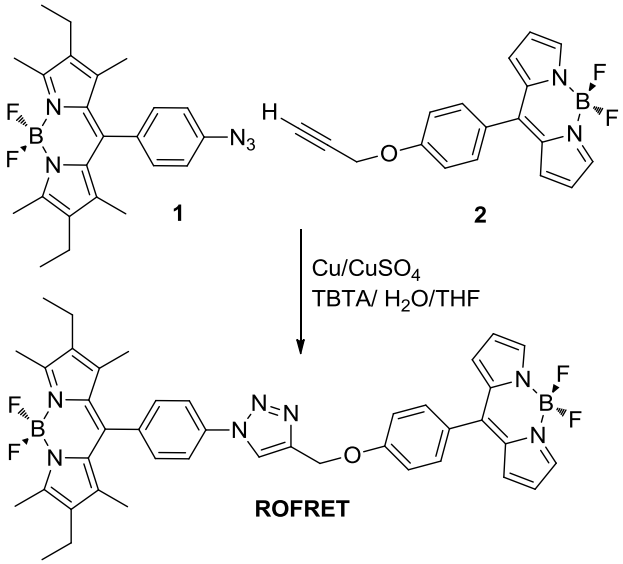

Scheme 2. Preparation of **ROFRET** using standard "click chemistry".

Preparation of ROFRET

To a two-necked round-bottomed flask (250 mL) equipped with a magnetic stirrer was added compound **1** (20 mg, 0.054 mmol, 1 eq) and THF (40 mL previously purged with N_2). To the mixture was added tris-[(1-benzyl-1H-1,2,3-triazol-4-yl)methyl]amine (TBTA) (6 mg, 0.011 mmol, 0.2 eq) and Cu (3 mg, 0.047 mmol, 1 eq). The reaction was stirred at 24 °C for 1 hour, then over 10 minutes an aqueous solution of $CuSO_4 \cdot 5H_2O$ (2 mg, 0.021 mmol, 0.4 equiv) in H_2O (50 ml) was added. Finally compound **2** (25 mg, 0.062 mmol, 1 eq) in THF (10 ml) was added over 10 minutes, and the reaction was stirred at 40 °C for 5 hours. The reaction was monitored by TLC until complete consumption of the starting material was observed. The aqueous layer was separated and extracted with CH_2Cl_2. The combined organics were dried ($MgSO_4$), filtered and removed on a rotary evaporator. Purification of the crude compound via column chromatography (SiO_2, eluant CH_2Cl_2 : petrol ether 50:50) and finally ethyl acetate afforded the desired product as a red solid. Yield (35 mg, 0.047 mmol, 87%). ^{1}H NMR (300 MHz, $CDCl_3$): δ = 0.89-0.94 (t, 6H), 1.27 (s, 6H), 2.20-2.28 (q, 4H), 2.48 (s, 6H), 5.36 (s, 2H), 6.48-6.49 (d, 2H), 6.90 (d, 2H), 7.13-7.16 (d, 2H), 7.42-7.45 (d, 2H), 7.50-7.53 (d, 2H); 7.86-7.87(d, 2H); 7.90 (s, 2H); 8.20 (s, 1H, triazo-H). ^{13}C NMR (75 MHz, $CDCl_3$): δ = 11.02, 11.56, 13.46, 16.13, 28.71, 29.70, 61.39, 114.06, 117.29, 119.92, 126.32, 129.45, 129.77, 130.32, 131.37, 131.51, 132.38, 134.05, 136.01, 136.43, 136.91, 1142.76, 143.84, 153.71, 159.79. ^{11}B NMR (128 MHz $CDCl_3$): δ = 0.0959; 0.1864; -0.4570; -0.6822; -0.9073 (quintet J = 34.6, 28.6 Hz). ^{19}F NMR (376 MHz $CDCl_3$): δ = -144.8861; -144.9544; -145.0283; -145.1023 (q, J = 28.6 Hz); δ = -145.5460; -145.6143; -145.6996; -145.7850 (q, J = 30.1 Hz). MALDI-MS calc. for $C_{41}H_{39}B_2N_7F_4O$ = 743.41 observed = 742$[M-H]^+$.

Acknowledgements

We thank Newcastle University for financial support and the Engineering and Physical Sciences Research Council (EPSRC) sponsored mass spectrometry service at Swansea for collecting the MADLI mass spectrum.

[1] a) C. R. Maldonado, L. Salassa, N. Gomez-Blanco, J. C. Mareque-Rivasb, *Coord. Chem. Rev.* **2013**, *257*, 2668-2688; b) Y.-P. Ho, K. W. Leong, *Nanoscale* **2010**, *2*, 60-68. c) K. K.-W. Lo, S. P.-Y. Li, K. Y. Zhang, *New J. Chem.* **2011**, *35*, 265-287; c) L. M. De Leeon-Rodriguez, A. J. M. Lubag, C. R. Malloy, G. V. Martinez, R. J. Gillies, D. Sherry, *Acc. Chem. Res.* **2009**, *42*, 948-957.

[2] a) L. Yuan, W. Lin, K. Zheng, S. Zhu, *Acc. Chem. Res.* **2013**, *46*, 1462-1473; b) M. K. Kuimova, G. Yahioglu, J. A. Levitt, K. Suhling, *J. Am. Chem. Soc.* **2008**, *130*, 6672-6673; c) M. K. Kuimova, *Chimia*, **2012**, *66*, 159-165; c) R. Cabot, C. A. Hunter, *Chem. Soc. Rev.* **2012**, *41*, 3485-3492.

[3] a) P. Lin, F. Yan, *Adv. Mater.* **2012**, *24*, 34-51. b) S. Shinoda, H. Tsukube, *Analyst*, **2011**, *136*, 431-435; c) U. Lange, N. V. Roznyatovskaya, V. M. Mirsky, *Anal. Chim. Acta.* **2008**, *614*, 1-26.

[4] C. Reichardt, *Pure Appl. Chem.* **2004**, *76*, 1903-1919.

[5] X.-d. Wang, O. S. Wolfbeis, R. J. Meier, *Chem. Soc. Rev.* **2013**, *42*, 7834-7869.

[6] a) Z. Guo, S.Park, J. Yoon, I. Shin, *Chem. Soc. Rev.* **2014**, *43*, 16-29; b) Z. Xu, J. Yoon, D. R. Spring, *Chem. Soc. Rev.* **2010**, *39*, 1996-2006.

[7] M. Burnworth, S. J. Rowan, C. Weder, *Chem.-Eur. J.* **2007**, *13*, 7828-7836.

[8] a) S.Yao, K. D. Belfield, *Eur. J. Org. Chem.* **2012**, 3199-3217; b) H. Koo1, M. S. Huh, J. H. Ryu, D.-E. Lee, I.-C. Sun, K. Choi, K. Kim, I. C. Kwon, *Nano Today* **2011**, *6*, 204-220.

[9] a) W. B. Frommer, M. W. Davidson, R. E. Campbell, *Chem. Soc. Rev.* **2009**, *38*, 2833-2841; b) L. Basabe-Desmonts, D. N. Reinhoudt, M. Crego-Calama, *Chem. Soc. Rev.* **2007**, *36*, 993-1017.

[10] a) G. Vereb, E. Jares-Erijman, P. R. Selvin, T. M. Jovin, *Biophys. J.* **1998**, *74*, 2210-2222; b) I. Hemmila, V. Laitala, *J. Fluorescence*, **2005**, *15*, 529-542.

[11] A. Gomes, E. Fernandes, J. L. F. C. Lima, *J. Biochem. Biophys. Methods* **2005**, *65*, 45-80.

[12] A. P. Demchenko, Y. Me´ly, G. Duportail, A. S. Klymchenko, *Biophys. J.* **2009**, *96*, 3461–3470.

[13] a) Z. Wang, X. Ding, S. Li, J. Shi, Y. Li, *RSC Advances* **2014**, 4, 7235-7245; b) J. M. Pagano, C. C. Clingman, S. P. Ryder, *RNA*, **2011**, *17*, 14-20.

[14] a) G. Bao, W. J. Rhee, A. Tsourkas, *Annu. Rev. Biomed. Eng.* **2009**, 11, 25–47.

[15] a) N. Boens, V. Leen, W. Dehaen, *Chem. Soc. Rev.* **2012**, *41*, 8212- ; b) A. C. Benniston, G. Copley, *Phys. Chem. Chem. Phys.* **2009**, *11*,4124-4131; R. Ziessel, A. Harriman, *Chem. Commun.* **2011**, *47*, 611-631.

[16] a) G. Ulrich, R Ziessel, A. Harriman, *Angew. Chem. Int Ed.* **2008**, *47*, 1184; b) A. Loudret, K. Burgess, *Chem. Rev.* **2007**, *107*, 4891-4932.

[17] H. L. Kee, C. Kirmaier, L. Yu, P. Thamyongkit, W. J. Youngblood, M. E. Calder, L. Ramos, B. Noll, D. F. Bocian, W. R. Scheidt, R. R. Birge, J. L. Lindsey, D. Holten, *J. Phys. Chem. B* **2005**, *109*, 20433-20443.

[18] a) M. A. H. Alamiry, A. C. Benniston, G. Copley, K. J. Elliott, A. Harriman, B. Stewart, Y.-G. Zhi, *Chem. Mater.* **2008**, *20*, 4024-4032. b) J. A. Levitt, P.-H. Chung, M. K. Kuimova, G. Yahioglu, Y. Wang, J. Qu, K. Suhling, *ChemPhysChem* **2011**, *12*, 662-672.

[19] a) A. Burghart, H. Kim, M. B. Welch, L. H. Thoresen, J. Reibenspies, K. Burgess, *J. Org. Chem.* **1999**, *64*, 7813-7819; b) G. J. Hedley, A. Ruseckas, A. Harriman, I. D. W. Samuel, *Angew. Chem. Int Ed.* **2011**, *50*, 6634-6637.

[20] S. E. Braslavsky, E. Fron, E., H. B. Rodriguez, E. S. Román, G. D. Scholes, G. Schweitzer, B. Valeur, J. Wirz, *Photochem. Photobiol Sci.* **2008**, *7*, 1444-1448.

[21] Nomenclature is derived from **RO**TOR and Fluorescence Resonance Energy Transfer (**FRET**) which describe the workings of the dyad.

[22] a) K. Sienicki, M. A. Winnik, *Chem. Phys.* **1988**, *121*, 163-174; b) P. Woolley, K. G. Steinhäuser, B. Epe, *Biophys. Chem*. 1987, *26*, 367-374; c) K. Sienicki, *J. Phys. Chem.* **1990**, *94*, 1944-1948.

[23] W. E. Ford, M. A. J. Rodgers, *J. Phys. Chem.* **1992**, *96*, 2917-2920.

[24] A. Harriman, M. Hissler, A. Khatyr, R. Ziessel, *Chem. Commun.* **1999**, 735-736.

[25] G. Ragazzon, P. Verwilst, S. A. Denisov, A. Credi, G. Jonusauskasc, N. D. McClenaghan, *Chem. Commun.* **2013**, *49*, 9110-9112.

[26] J. E. Moses, A. D. Moorhouse, *Chem. Soc. Rev.* **2007**, *36*, 1249-1262.

[27] Gaussian 03, M. J. Frisch, G. W. Trucks, H. B. Schlegel, G. E. Scuseria, M. A. Robb, J. R. Cheeseman, J. A. Montgomery, Jr., T. Vreven, K. N. Kudin, J. C. Burant, J. M. Millam, S. S. Iyengar, J. Tomasi, V. Barone, B. Mennucci, M. Cossi, G. Scalmani, N. Rega, G. A. Petersson, H. Nakatsuji, M. Hada, M. Ehara, K. Toyota, R. Fukuda, J. Hasegawa, M. Ishida, T. Nakajima, Y. Honda, O. Kitao, H. Nakai, M. Klene, X. Li, J. E. Knox, H. P. Hratchian, J. B. Cross, V. Bakken, C. Adamo, J. Jaramillo, R. Gomperts, R. E. Stratmann, O. Yazyev, A. J. Austin, R. Cammi, C. Pomelli, J. W. Ochterski, P. Y. Ayala, K. Morokuma, G. A. Voth, P. Salvador, J. J. Dannenberg, V. G. Zakrzewski, S. Dapprich, A. D. Daniels, M. C. Strain, O. Farkas, D. K. Malick, A. D. Rabuck, K. Raghavachari, J. B. Foresman, J. V. Ortiz, Q. Cui, A. G. Baboul, S. Clifford, J. Cioslowski, B. B. Stefanov, G. Liu, A. Liashenko, P. Piskorz, I. Komaromi, R. L. Martin, D. J. Fox, T. Keith, M. A. Al-Laham, C. Y. Peng, A. Nanayakkara, M. Challacombe, P. M. W. Gill, B. Johnson, W. Chen, M. W. Wong, C. Gonzalez, J. A. Pople, Gaussian, Inc., Wallingford CT, 2004.

[28] K. Krumova, G. Cosa, *J. Am. Chem. Soc.* **2010**, *132*, 17560–17569.

[29] G. D. Scholes, *Annu. Rev. Phys. Chem.* **2003**, *54*, 57-87.

[30] To take into account the fact that energy transfer can take place over different separation distances the equation can be modified to:

$P(R_0) = \int_0^\infty dR\, f(R) \frac{R_0^6}{R_0^6+R^6}$ where *f(R)* is a distance distribution function, see

for example, C. R. Cantor, P. Pechukas, *Proc. Nat. Acad. Sci.* **1971**, *68*, 2099-2101; A. Grinvald, E. Haas, I. Z. Steinberg, *Proc. Nat. Acad. Sci.* **1972**, *68*, 2099-2277.

[31] The average value of $\kappa^2 = 0.66$ was used in calculations since the two Bodipy groups are assumed to sample many different geometries in fluid solution. Using values of n for solvents may be again an over simplification since there are several papers discussing the validity of the approximation, see for example: R. S. Know, H. van Amerongen, *J. Phys. Chem. B* **2002**, *106*, 5289-5293.

[32] a) I. Gryzynsiu, W. Wiczk, M. L. Johnson, J. R. Lakowicz, *Chem. Phys. Lett.* **1988**, *145*, 439-446; b) B. Valeur, J. Mugnier, J. Pouget, J. Bourson, F. Santi, *J. Phys. Chem.* **1989**, *93*, 6073-6079; c) M. Kasche, N. P. Ernsting, B. Valeur, j. Bourson, *J. Phys. Chem.* **1990**, *94*, 5757-5761; d) S. Sindbert, S. Kalinin, H. Nguyen, A. Kienzler, L. Clima, W. Bannwarth, B. Appel, S. Muller, C. A. M. Seidel, *J. Am. Chem. Soc.* **2011**, *133*, 2463-2480; J. M. Beecham, E. Haas, *Biophys. J.* **1989**, *55*, 1225-1236.

[33] a) S. Chatterjee, S. Nandi, S. Chandra, C. Bhattacharya, *J. Photochem. Photobiol. A: Chem.* **2005**, *173*, 221-227; b) J. A. Mondal, G. Ramakrishna, A. K. Singh, H. N. Ghosh, M. Mariappan, B. G. Maiya, T. Mukherjee, D. K. Palit, *J. Phys. Chem. A* **2004**, *108*, 7843-7852.; c) D. Wang, E. Geva, *J. Phys. Chem.* B **2005**, *109*, 1626-1634; d) A. F. Vaudolb, D. M. Hercules, *J. Am. Chem. Soc.* **1971**, *93*, 2599-2602.

[34] G. Srinivas, A. Yethiraj, B. Bagchi, *J. Chem. Phys.* **2001**, *114*, 9170-9178.

[35] M. A. Haidekker, T. P. Brady, D. Lichlyter, E. A. Theodorakis, *J. Am. Chem. Soc.* **2006**, *128*, 398-399.

[36] a) R. Ziessel, G. Ulrich, A. Harriman, M. A. H. Alamiry, B. Stewart, P. Retailleau, *Chem.-Eur. J.* **2009**, *15* 1359-1369; b) K. Rurack, M. Kollmannsberger, J. Daub, *New J. Chem.* **2001**, *25*, 289-292.

[37] a) A. C. Benniston, G. Copley, K. J. Elliott, R. W. Harrington, W. Clegg, *Eur. J. Org. Chem.* **2008**, 2705-2713; b) Z-N. Sun, H.-Li Wang, F.-Q. Liu, Y. Chen, P. K. H. Tam, D. Yang, *Org. Lett.* **2009**, *11*, 1887-1890; c) Z.-N. Sun, F.-Q. Liu, Y. Chen, P. K. H. Tan, D. Yang, *Org. Lett.* **2008**, *10*, 2171-2174.

Received: ((will be filled in by the editorial staff))
Revised: ((will be filled in by the editorial staff))
Published online: ((will be filled in by the editorial staff))